JOURNAL OF MATERIALS SCIENCE **34** (1999) 1031–1035

Microstructural and electrical properties of sintered tungsten trioxide

A. G. SOUZA FILHO, J. G. N. MATIAS, N. L. DIAS, V. N. FREIRE
Departamento de Física, Universidade Federal do Ceará, Campus do Pici. Caixa Postal 6030, 60451-970 Fortaleza, Ceará, Brasil

J. F. JULIÃO
Núcleo de Pesquisas Tecnológicas, Universidade de Fortaleza Av. Washington Soares, 1321, Caixa Postal 1258, 60811-341 Fortaleza, Ceará, Brasil
E-mail: juliao@feq.unifor.br

U. U. GOMES
Departamento de Física Teórica e Experimental, Universidade Federal do Rio Grande do Norte CEP: 59072910 Natal, Rio Grande do Norte, Brasil

Tungsten trioxide sintered wafers were prepared from WO_3 powder obtained when ammonium paratungstate is decomposed in air at moderate temperature. Two wafer series of five samples were sintered under the same conditions in the temperature range 600–1000 °C. One of these wafers series was submitted to a subsequent annealing at 700 °C under a hydrogen atmosphere. All samples were characterized at room temperature by X-ray diffraction and electrical measurements. X-ray spectra show that WO_3 ceramic presents a mixture of the triclinic and monoclinic phases before the reduction process. After the reduction process, WO_2 and four hydrogen tungsten bronze phases are present in wafers. Capacitance measurements showed that the samples submitted only to the sintering process changed the dielectric constant with the frequency according to the Debye model. The reduced WO_3 shows a semiconductor behavior, as determined by electrical resistivity measurements.

1. Introduction

Tungsten trioxide (WO_3) has many technological applications. As thin films, it is used extensively in eletrochromic devices [1], for solar energy conversion and photovoltaic water purification [2], and in surface acoustic wave gas sensors [3]. WO_3 films may be prepared by several different techniques: sol-gel [4], spray pyrolysis deposition [5], thermal evaporation [6], r.f. sputtering [7], anodization [8] and e-beam deposition [9], for example. Several studies in compacted WO_3 ceramics have been reported in the literature, mainly due to its importance in the fabrication of gas sensors [10, 11]. Recently, ceramic semiconductors have been used for detection and control of toxic gases [11]. Consequently, as others metal oxides, such as SnO_2, TiO_2, and Fe_2O_3, doped WO_3 is a basic material for use in devices that find applications related to environmental protection.

Due to their high dielectric constant, WO_3 sintered wafers are suitable for the fabrication of ceramic capacitors. The changes in the electrophysical properties of the stable and metastable WO_3 ceramic wafers related to γ-ray doses and temperature variation in the range 180–300 K was reported by Soshnikov *et al*. [12]. These authors have described the dielectric of the WO_3 ceramic at low frequency (1.0 Hz) as a function of the temperature variation and have observed a monoclinic to triclinic phase transition in the temperature interval 200–230 K, and also a triclinic to monoclinic phase transition around 300 K. Pfeifer *et al*. [13] studied the dielectric properties of tungsten trioxide at high frequency (60 MHz to 9.44 GHz). However, literature reports on the dielectric response of WO_3 sintered wafers at room temperature to low frequency oscillating fields are very scarce.

Since the technological interest in the WO_3 ceramic is growing, it seems opportune to pursue a better understanding of its properties to improve its characterization. The aim of the present work is to study the microstructural and electrical properties of the WO_3 ceramic obtained by compressing the WO_3 powder. Measurements at room temperature performed before and after the reduction process of WO_3 ceramic samples were carried out. The dielectric constant behavior of the WO_3 ceramic as a function of the signal frequency in the range 120 Hz–10 KHz is presented, as its X-ray diffratograms, and the sintering temperature dependence of its electrical resistivity.

2. Experimental

WO_3 ceramic samples were prepared from the WO_3 powder obtained after ammonium paratungstate

thermal decomposition in room atmosphere. The WO_3 powder of grain size 75 μm was submitted to a hydrostatic pressure of 400 MPa. Two groups of WO_3 wafers with 10 mm diameter and 5 mm of thickness were sintered in air in the temperature range 600–1000 °C.

One group of WO_3 samples was submitted to a physical-chemical reduction process in a H_2 atmosphere. The furnace temperature during the physical-chemical reduction process was maintained at 700 °C for 120 min. Such a process was carried out in a chamber where the reducing atmosphere was kept under a hydrogen flux of 18 ml min^{-1}, based on previous studies made by da Silva [14] on this material.

Both groups of WO_3 samples were microstructurally characterized by X-ray diffraction, using a RIGAKU diffractometer, model DMAXB, with a CuK_α radiation of 0.1504 nm wavelength, coupled to a RIGAKU computer FP 6000. The X-ray tube has a 40 kV operating voltage and a 20 mA current. All measurements were performed within the 20° to 80° angular interval with a 6° min^{-1} goniometer velocity. The Joint Committee on Powder Diffraction Standard (JCPDS) cards were used to identify the chemical species and their phases [15].

To perform the electrical characterization the wafers were superficially metallized with silver paste. Measurements of the electric capacitance were made in the group of unreduced WO_3 samples with a HP capacitance bridge model 4262-A RCL Meter. Using these results and the circular parallel plates capacitor model, the dielectric constant was obtained.

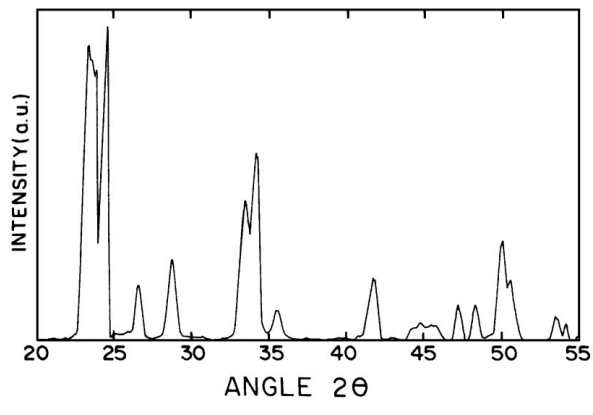

Figure 1 X-ray spectrum of the WO_3 original powder used to fabricate wafers (da Silva [14]).

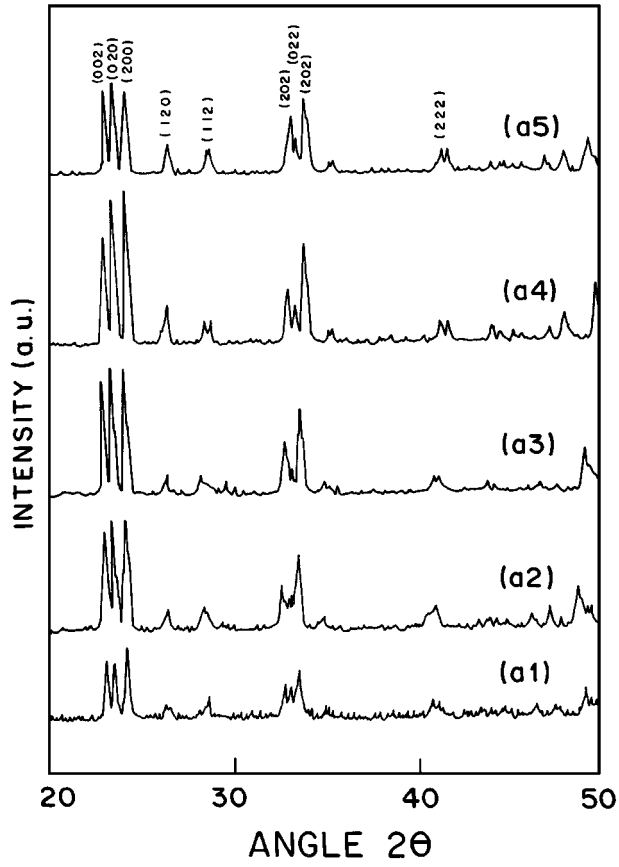

Figure 2 X-ray diffraction spectra of WO_3 sintered wafers at (a1) 600 °C, (a2) 700 °C, (a3) 800 °C, (a4) 900 °C and (a5) 1000 °C.

3. Results and discussion

3.1. X-ray measurements

The X-ray diffraction spectrum of WO_3 starting powder used in our experiment is shown in Fig. 1. The JCPDS card suggests from this spectrum that WO_3 has crystallized in the monoclinic phase. This result is in accordance with the literature [16].

When commercial WO_3 powder is submitted to pressure for the production of the WO_3 ceramic samples, some of their covalent chemical bonds can be destabilized and the structural transitions that take place are affected. Soshnikov *et al.* [12] has determined that WO_3 powder submitted to high pressures exhibits a triclinic phase at room temperature. These authors attributed the displacement of the transition temperature between triclinic and monoclinic phases to the presence of cobalt ions in the WO_3 powder utilized for the preparation of disk-shaped samples. The pellets used by those authors were compressed at a pressure of 7.0×10^4 MPa.

The influence of the sintering temperature of WO_3 ceramic on X-ray spectra is shown in Fig. 2. The three peaks of highest intensity are related to the triclinic phase with (0 0 2), (0 2 0), and (2 0 0) spatial orientation. Other peaks assigned in the spectra correspond to the monoclinic phase. This result indicates the existence of monocrystals formed from the monoclinic phase of WO_3 powder. The mixture of phases present in our results may be attributed to the application of a moderate pressure on the process of WO_3 wafers fabrication. We assume that the pressures used in the fabrication of our samples were not sufficient to completely convert the monoclinic to triclinic WO_3.

Fig. 3 shows X-ray diffraction spectra of reduced WO_3 ceramic as a function of sintering temperature. The majority peaks of WO_3 have disappeared and new peaks appeared after the reduction process of WO_3 ceramic. This result is similar to that reported in the literature [17–19], and are attributed by those authors to the suboxide WO_2 and hydrogen tungsten bronze H_xWO_3, where x presented the following values: 0.1, 0.23, 0.33, and 0.5. The new chemical species are identified in the literature [17–19] as being tetragonal $H_{0.1}WO_3$, tetragonal $H_{0.23}WO_3$, tetragonal $H_{0.33}WO_3$, and cubic $H_{0.5}WO_3$.

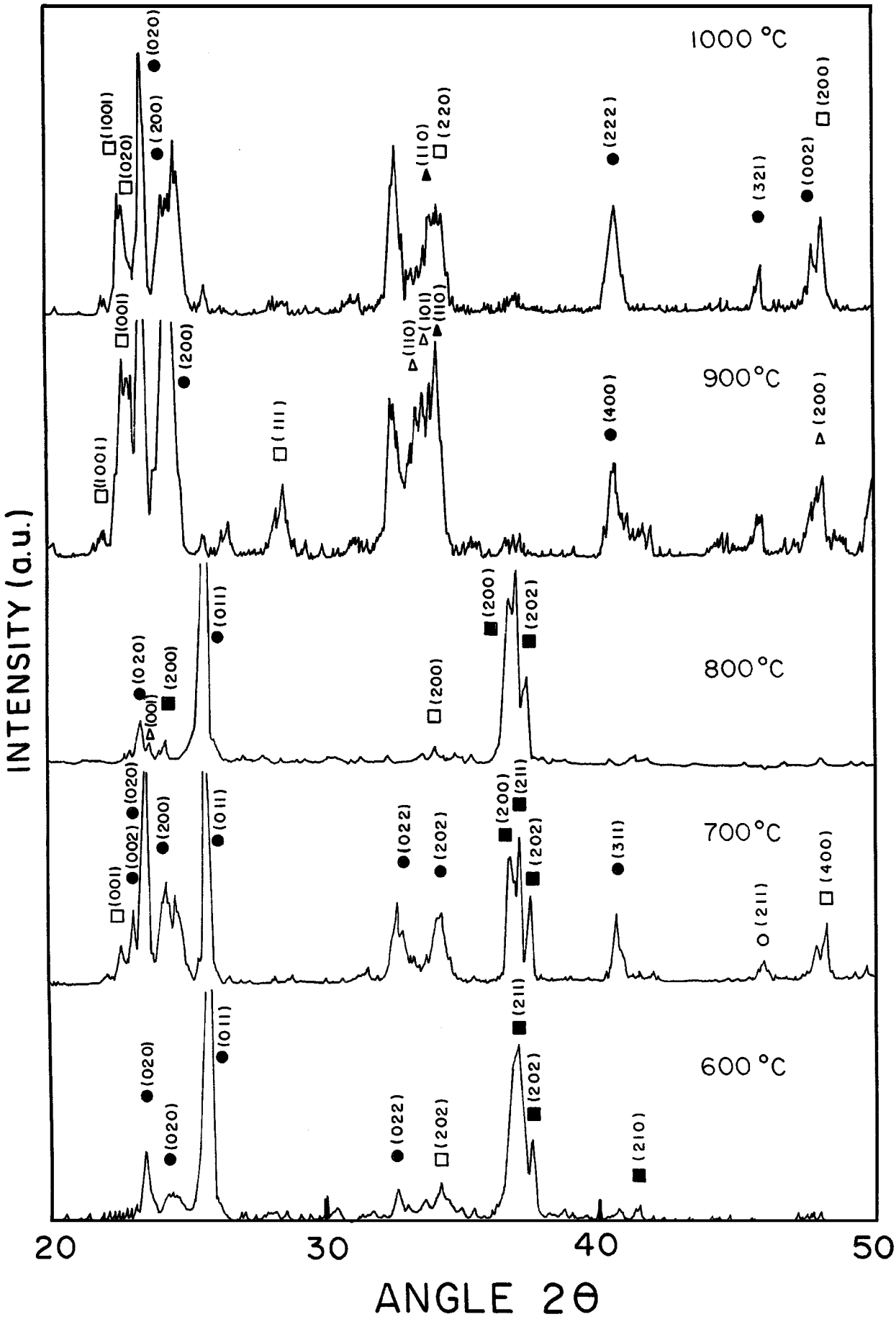

Figure 3 X-ray diffraction spectra of several WO_3 samples, sintered at 600 °C, 700 °C, 800 °C, 900 °C and 1000 °C. These samples were also reduced at 700 °C in a H_2 atmosphere; ● (WO_3), I (WO_2), ○ ($H_{0.1}WO_3$), ($H_{0.23}WO_3$), △ ($H_{0.33}WO_3$) and ▲ ($H_{0.5}WO_3$).

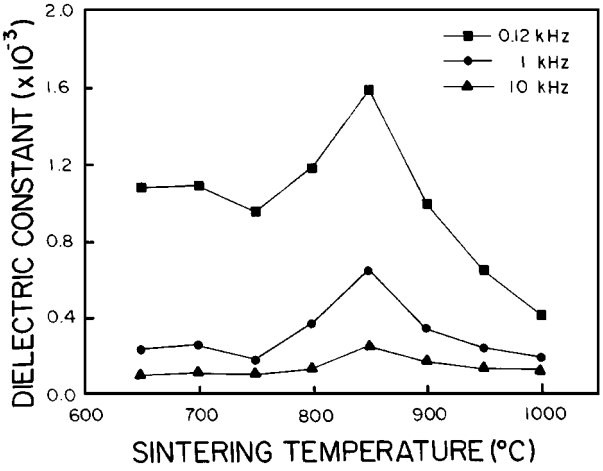

Figure 4 Dielectric constant of WO_3 sintered wafers as a function of sintering temperature.

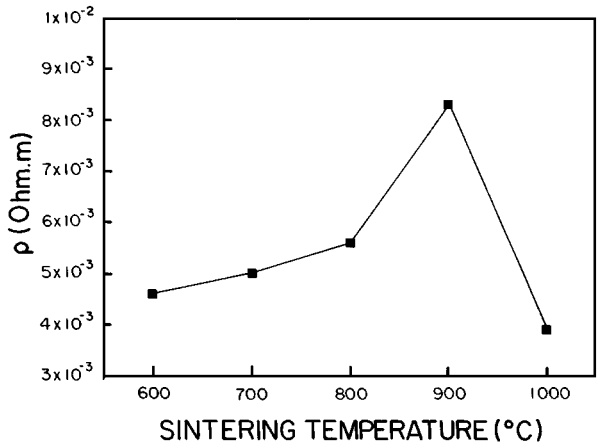

Figure 5 Electrical resistivity of WO_3 sintered at several temperatures and reduced at 700 °C in the presence of hydrogen atmosphere.

3.2. Electrical measurements

Fig. 4 shows the relative dielectric constant as a function of the sintering temperature, for three different values of frequency measured at room temperature. Independently of the sintering temperature, the dielectric constant decreases with increasing frequency of the signal used in the measurements. This result is similar to that reported in perovskite glass-ceramic [20]. The influence of sintering temperature on the dielectric constant is such that it varies slowly between 600 °C and 750 °C, presenting a peak at 850 °C. Between 850 °C and 1000 °C there is a decrease in the value of the dielectric constant. To understand this result we report on the effects of temperature on the dielectric constant, as described by Debye relations. The real and imaginary parts of the dielectric constant are given by the following relations:

$$\varepsilon_r = \varepsilon_\infty + \frac{\varepsilon_{(0)} - \varepsilon_\infty}{1 + \omega^2\tau^2}, \tag{1}$$

$$\varepsilon_i = \frac{[\varepsilon_{(0)} - \varepsilon_\infty]\omega\tau}{1 + \omega^2\tau^2}, \tag{2}$$

where, ε_∞ is the dielectric constant at optical frequency, $\varepsilon_{(0)}$ the static dielectric constant, ω the measuring frequency, and τ is the relaxation time. The relaxation time τ is a function of temperature. From Equation 1 it is clear that ε_r decreases when the frequency ω increases. We have assumed that the same relation is valid when T is the sintering temperature, due to the coalescence between grains of WO_3 powder induced by the sintering process. Therefore, for a constant value of frequency, there is an increase of the dielectric constant as the sintering temperature increases. Furthermore, the dielectric response is not only a function of the relaxation time. Other mechanisms have an influence on the dielectric constant, such as the space charge polarization and the number of interfaces. It is well known that the sintering process produces microstructural defects in the materials, such as number of vacancies, vacancy groups and grain boundaries, for example. As a consequence, there will be a small migration of ions by the action of an a.c. electric field that results in a weak polarization of both W^{6+} and O^{2-} ions when a higher sintering temperature is used, thus decreasing the dielectric constant. Based on these considerations, the peak of the dielectric constant that appears at 850 °C may be explained by two combined effects: The increasing dielectric constant, due to relaxation time, and the decreasing dielectric constant due to the weak polarization.

Another explanation for this peak can be obtained by examining the X-ray diffraction pattern shown in Fig. 2. These results indicate that there is a major cristallinity around 850 °C, that may be determined by the structure factor, i.e. there is a greater number of induced dipoles in a preferential spatial orientation, resulting in a maximum value of the dielectric constant. This explanation takes into account the fact that the intensity of the X-ray beam scattered in this situation depends only on the structure factor. We assume that parameters such as temperature factor, Lorentz factor, polarization, multiplicity factor, and temperature, are invariant to each WO_3 ceramic sample characterized.

Reduced WO_3 ceramic was electrically characterized by resistivity measurements. Fig. 5 shows the influence of sintering temperature on the resistivity of reduced WO_3 ceramic at 700 °C in H_2 atmosphere. The same behavior was observed in the range of frequency studied with no dispersion in the resistivity value. These samples presented electrical resistivity in the range 10^{-3} Ω m to 10^{-2} Ω m, that may be caused by the presence of hydrogen tungsten bronze. The transition of this material from insulator to semiconductor is attributed to the intercalation of the H^+ ions in the oxygen vacancies and tungsten interstitial positions [21].

4. Conclusions

The behavior of the dielectric constant of WO_3 sintered wafers is explained by extrinsic factors, i.e. microstructural defects and coalescence of grains. Combining these arguments with the Debye relation, it is possible to understand the spectrum of dielectric constant as a function of sintering temperature. The analysis of X-ray diffratograms shows a mixture of triclinic and monoclinic phases of WO_3 with preferential growth

orientation on directions (0 0 2), (0 2 0), and (2 0 0) which are related to the triclinic phase. After the reduction process, the X-ray spectra show the presence of WO_2 and tungsten bronze in four phases. These new phases give the material semiconducting properties which are confirmed by electrical resistivity measurements.

Acknowledgements

The authors are very grateful to MSc J. A Freitas e Silva for his collaboration in the X-ray measurements. This work received partial support from the Conselho Nacional de Desenvolvimento Científico e Tecnológico, CNPq Brazil.

References

1. S. PASSERINI, R. PILLEGI and B. SCROSATI, *Eletrochim. Acta* **37** (1992) 1703.
2. S. HOTHANDANI, I. BEDJA, R. S. FESSENDU and P. V. KAMAT, *Langmuir* **10** (1994) 17.
3. M. D. ANTONIK, J. E. SCHNEIDER, E. L. WITTMAN, K. SNOW, J. F. VETELINO and R. D. LOD, *Thin Solid Films* **256** (1995) 247.
4. J. P. CRONIN, D. J. TARICO, J. C. L. TONAZZI, A. AGRAWAL and S. R. KENNEDY, *Sol. Energy Mater.* **29** (1993) 371.
5. JIANPING ZHANG, SILVIA A. WESSEL and KONARD COLBOW, *Thin Solid Films* **185** (1990) 265.
6. O. BONHKE, C. BONHKE and G. ROBERT, *Solid State Ion.* **6** (1982) 121.
7. HOSSAIN AKRAM, HIROKAZU TATSUOCA, MICHIHIKO KITAO and SHOJI YAMADA, *J. Appl. Phys.* **65** (1987) 2039.
8. A. DIPAOLA, F. DIQUATRO and C. SUNSERI, *J. Eletrochem. Soc.* **125** (1978) 1344.
9. S. A. AGNIHOTRY, RASHNI, R. RAMCHANDRAN and S. CHANDRA, *Sol. Energy Mater.* **36** (1995) 289.
10. H. TORVELA, T. TAAKOLA, A. UUSINAK and S. LEPPAVUORI, *J. Electron. Mater.* **15** (1986) 7.
11. K. S. PATEL and H. T. SUN, *Key Eng. Mater.* **115** (1996) 181.
12. L. E. SOSHNIKOV, S. I. URBANOVICH and N. F. KURILOVICH, *Phys. Solid State* **37** (1995) 1674.
13. J. PFEIFER, I. CSABA and K. ELEK, *J. Solid State Chem.* **111** (1994) 349.
14. G. DA SILVA, MSc Thesis, DFTE, Natal-RN Brazil (1995).
15. "Powder Diffraction File Manual," (Joint Commitee on Powder Diffraction Standards).
16. H.-T. SUN, C. CANTAALINI, L. LOZZI, M. PASSACANTANDO, S. SANTUCCI and M. PELINO, *Thin Solid Films* **287** (1996) 258.
17. B. AMPE, J. M. LEROY, D. THOMAS and G. TRIDOT, *Rev. Chim. Miner.* **5** (1968) 801.
18. P. G. DICKENS and R. J. HURDICH, *Nature* **215** (1967) 1266.
19. B. S. HOBBS and A. C. C. TSEUNG, *J. Eletrochem. Soc.* **119** (1972) 580.
20. JIIN-JYN SHYU and YEONG-SONG YANG, *J. Mater. Sci.* **31** (1996) 4859.
21. M. GREEN, *Thin Solid Films* **50** (1978) 150.

Received 17 April
and accepted 19 August 1998